Core–Shell Materials

DOI: 10.1002/ange.200804167

Microcontainers with Fluorescent Anisotropic Zeolite L Cores and Isotropic Silica Shells**

Andrés Guerrero-Martínez, Sandra Fibikar, Isabel Pastoriza-Santos, Luis M. Liz-Marzán, and Luisa De Cola**

The organization of photophysically active units in nanostructures gives rise to collective effects that can be used for the design of new functional materials.[1] Various strategies have been followed to achieve organized multichromophoric systems, ultimately leading to the development of photoactive polymers,[2] dendrimers,[3] self-assembled monolayers,[4] and mesoporous silica structures.[5] Among them, zeolite L crystals have emerged as potential new components for artificial antenna devices,[6] for self-assembly in functional supramolecular systems,[7] and even as connecting units between living organisms.[8] Zeolite L is a crystalline porous material consisting of interlocking tetrahedrons of silica and alumina, which form unidirectional channels along the *c* axis of the hexagonal crystal structure that contain cations to compensate the negative charge of the alumina framework.[9] Owing to its characteristic rigid and optically transparent structure and its porosity, with channels that present an opening of 0.71 nm and a largest internal free diameter of 1.26 nm, zeolite L is often used as a host matrix for highly luminescent dye molecules that can fit inside the channels.[10] These organic dyes can be inserted into the crystals by well-known procedures, such as insertion from the gas phase or by ion exchange,[6] thus preventing, in some cases, their self-aggregation in solution and superimposing a specific organization with a high concentration of monomers.[11] However, this inclusion phenomenon is a thermodynamically reversible process, and the use and manipulation of dye-loaded zeolite L crystals in solution is restricted by the solubility of the inserted molecules in the corresponding solvent.[12] Therefore, leakage of the dye molecules is often observed, especially for cationic molecules in water or under physiological conditions, which prevents their possible use in biomedical applications. To avoid the escape of molecules out of zeolite L crystals, the channel entrances can be blocked using different types of stopcock molecules, based on reversible or irreversible processes such as surface adsorption or covalent bonding, respectively.[13] However, these procedures have some drawbacks, including the chemical modification of the crystal surface, the time-consuming synthesis demanded by the preparation and binding of the stopcock molecules, and the typically low yields. Therefore, suitable coatings for zeolite L systems are needed to overcome such limitations. These coatings should endow the crystals with several beneficial properties, such as the possibility of subsequent functionalization, biocompatibility, enhanced colloidal stability under different temperatures and in various solvents, and a suitable hydrophilicity.

Silica has long been appreciated as the material of choice for coating a wide variety of colloids and nanoparticles as a means to improve their technological applications in catalysis, photonics, electronics, optics, and biomedicine.[14] Several methods have been reported over the past decade for silica coating of colloids and nanoparticles, including sol–gel (Stöber process)[15] and aerosol pyrolysis,[16] among others.[17] Since the composition of zeolite L includes silica subunits, coating with a silica shell is possible. In fact, the preparation of materials with controlled porosity using zeolite nanoparticles within a mesoporous silica matrix has been recently described.[18] However, to our knowledge, proper encapsulation of zeolites within silica shells to achieve single multicomposite objects has not been reported.

The zeolite/silica system could be a multifunctional material, as it would: 1) protect the dye molecules encapsulated inside the zeolite channels from interaction with solvent and leakage; 2) allow the construction of multicolor systems in which different dyes can be entrapped in the zeolite and in the silica shell; 3) preserve the anisotropic fluorescence of the channel-entrapped dyes (inside the zeolites) and the isotropic emission of the dyes encapsulated in the silica network.[19,20] This last property, which cannot be achieved in multishell silica particles, can be used to construct nano- and microscale materials in which the coexistence of both anisotropic and isotropic fluorescence can be employed for imaging and photonic applications.

We report herein a silica-coating procedure that has been devised for coating zeolite L crystals but which can be readily extended to other zeolite types and to honeycomb mesoporous silica materials. The initial wrapping strategy was based on a direct hydrolysis and condensation of tetraethoxysilane (TEOS)[15] in an ethanol–water suspension of zeolite L (Scheme 1), leading to growth of homogeneous silica shells.

[*] Dr. A. Guerrero-Martínez, S. Fibikar, Prof. Dr. L. De Cola
Physikalisches Institut and Center for Nanotechnology (CeNTech)
Westfälische Wilhelms-Universität Münster,
Heisenbergstrasse 11, 48149 Münster (Germany)
Fax: (+49) 251-980-2834
E-mail: aguerrero@quim.ucm.es
decola@uni-muenster.de
Dr. I. Pastoriza-Santos, Prof. Dr. L. M. Liz-Marzán
Departamento de Quimica Fisica and Unidad Asociada CSIC,
Universidade de Vigo (Spain)

[**] Financial support by the Spanish Ministerio de Educación y Ciencia (A.G.M. and project NAN2004-08843) is gratefully acknowledged. J.B. Rodríguez-González and C. Serra (CACTI, Univ. Vigo) and nanoAnalytics (CeNTech, Münster) are thanked for assistance with SEM and fluorescence microscopy measurements, respectively.

Supporting information for this article is available on the WWW under http://dx.doi.org/10.1002/anie.200804167.

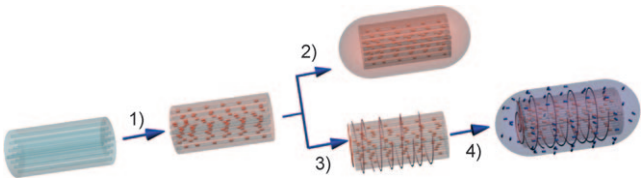

Scheme 1. Illustration of the two processes used to obtain fluorescent multicolor nanocontainers based on zeolite L crystals coated with silica shells. Dye molecules are inserted into the zeolite L crystals from the gas phase or through ion exchange (1) with subsequent basic silica condensation (2). Alternatively, the silica shell can be constructed by polyelectrolyte layer-by-layer assembly (3) and subsequent silica condensation, which may be performed in the presence of a cationic dye (4).

Subsequently, this protocol was improved through a combination of the polyelectrolyte layer-by-layer technique (LBL)[21] and TEOS hydrolysis and condensation (Scheme 1). Our study focused on the preparation of isolated, fluorescent, multicolor capsules in which the zeolite core and the silica shell present anisotropic and isotropic luminescence, respectively.

The selected cylindrical 1 μm long zeolite L crystals were prepared according to a published procedure.[22] As an initial strategy to synthesize silica-coated zeolite L (Zeo@SiO_2), we followed the well-known Stöber method for silica coating (Scheme 1). The resulting material was analyzed by transmission and scanning electron microscopy (TEM and SEM; Figure 1), thus demonstrating the effectiveness of this method for silica shell growth. For thin shells, the characteristic, well-defined edges and terraces of the zeolite L crystals become smoother. Upon further TEOS condensation, some surface roughness is observed, likely owing to the fast growth of silica under the selected experimental conditions. The coating thickness was estimated using X-ray photoelectron spectroscopy (XPS, see survey XPS spectra in the Supporting Information). Figure 2 shows different regions of the XPS spectra of zeolite and Zeo@SiO_2 crystals dried on a Si wafer. The analysis of XPS regions corresponding to 95–110 eV and 68–85 eV shows that the sample contains silicon oxide (Si 2p, 103.4 eV) and aluminum oxide (Al 2p, 76.2 eV), which arise from the characteristic silica and alumina tetrahedrons of the zeolite structure. A broad, intense signal is observed around 100 eV that can be assigned to elemental Si 2p1 and Si 2p3 from the substrate. Evidence in favor of the core–shell structure is provided by the analysis of the silica-coated sample. From Figure 2b it is clear that after two TEOS condensation steps, the peak corresponding to aluminum oxide has completely disappeared, indicating the formation of a coating layer thicker than 4–5 nm.[23]

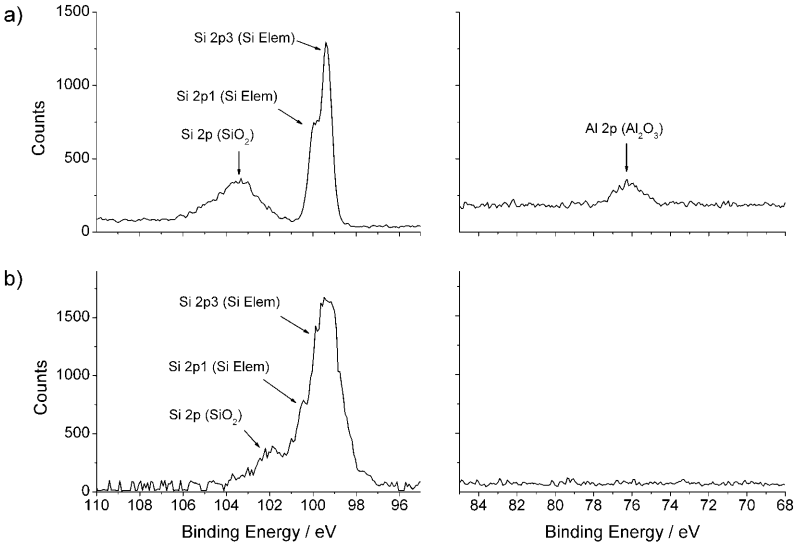

Figure 2. XPS spectra of a) the original zeolite L crystals and b) Zeo@SiO_2. Left silicon regions; right aluminum regions.

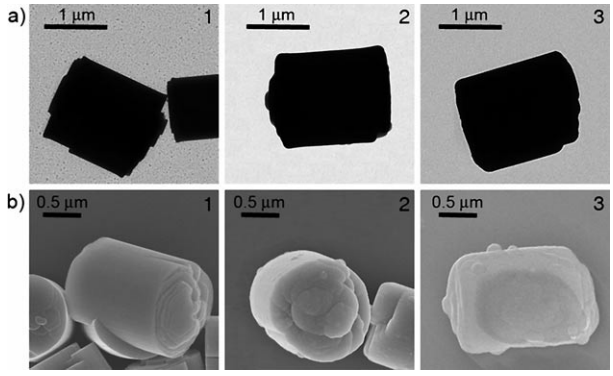

Figure 1. a) Transmission and b) scanning electron micrographs of zeolite L crystals. 1) Zeolite L; 2,3) silica-coated zeolite L crystals Zeo@SiO_2. The silica shell thickness increases from (2) to (3).

The crystals shown so far were empty, meaning that the channels contain only solvent molecules and ions. However, they can be filled with dye molecules prior to the coating process. For example, insertion into zeolite L of the neutral dye *N*,*N*′-bis(2,6-dimethylphenyl)perylene-3,4,9,10-tetracarboxylic diimide (DXP) to form Zeo(DXP)@SiO_2 or of the cationic dye Oxazine 1 ($Ox1^+$) to form Zeo($Ox1^+$)@SiO_2 and subsequent silica coating results in different core–shell building blocks.

No significant changes were observed in the emission and excitation profiles of the dyes between uncoated and coated zeolites (see the Supporting Information). The porosity of the silica layers in Zeo(DXP)@SiO_2 and Zeo($Ox1^+$)@SiO_2 was examined in dichloromethane (DCM) and ethanol, respectively. To this end, the release of dye entrapped inside the zeolite was measured using the absorbance of the filtered supernatant solutions after 24 h of stirring (see the Supporting Information). The UV/Vis measurements revealed that leakage of the encapsulated dyes was twelve and ten times lower (for Zeo(DXP)@SiO_2 and Zeo($Ox1^+$)@SiO_2, respectively) than from the corresponding uncoated zeolite samples.

From these results we conclude that, although the dye leakage was hindered, the coated systems were not completely isolated from the external medium. Moreover, we cannot exclude the incorporation of leaked dye from zeolite L crystals into the silica layer during the Stöber synthesis, especially in the case of $Ox1^+$, which is highly soluble in ethanol. The coatings prepared with two TEOS condensation steps seem to lead to structures with lower luminescence intensity than the uncoated samples.

To further restrict the release of inserted molecules, we decided to use the LBL technique prior to application of the Stöber process (Scheme 1).[24] Because the zeolite L crystals possess a low negative surface charge (zeta potential, $\zeta = -35$ mV), LBL wrapping with positive polyelectrolyte chains is strongly favored. After dye loading, zeolite L crystals were dispersed in water and mixed with an aqueous solution of a positive polyelectrolyte (poly(allylamine hydrochloride), PAH). A single polyelectrolyte layer was found to completely screen and reverse the negative charge of natural zeolite L crystals ($\zeta = +30$ mV). Then, poly(vinylpyrrolidone) (PVP), which is slightly negatively charged under these experimental conditions, was used to partly screen the surface charge ($\zeta = +10$ mV), allowing transfer into ethanol and subsequent silica coating through the Stöber method.[24] The resulting silica shell provides the coated zeolite L crystals with a negative charge ($\zeta = -28$ mV). The transmission and scanning electron micrographs of the coated samples (Zeo(DXP)@PAH/PVP@SiO_2 and Zeo($Ox1^+$)@PAH/PVP@SiO_2) were analogous to those depicted in Figure 1. Furthermore, XPS analysis of these samples showed results equivalent to those in Figure 2, again confirming that shells thicker than 4–5 nm were obtained after two TEOS condensation steps. No significant changes were observed in the emission and excitation profiles of the crystals after LBL adsorption and subsequent silica coating (see the Supporting Information). UV/Vis measurements of supernatant solutions from Zeo(DXP)@PAH/PVP@SiO_2 in DCM and Zeo($Ox1^+$)@PAH/PVP@SiO_2 in ethanol after 24 h of stirring indicated that there was no leakage of dye molecules from the channels (see the Supporting Information). These results indicate the formation of isolated nanocomposite capsules in which the polyelectrolyte layers act as steric and electrostatic barriers isolating the zeolite system from the external environment through an impermeable silica coating.[25]

Additionally, the silica coating on not-loaded zeolite L crystals was prepared through LBL assembly and two TEOS condensation steps in the presence of the cationic dye 4′,6-diamidino-2-phenylindole ($DAPI^+$). The resulting crystals contain the fluorescent molecules embedded within the amorphous silica layer. In toluene solutions they show the characteristic unstructured excitation and emission bands of the chromophore (Zeo@PAH/PVP@SiO_2($DAPI^+$), $\lambda_{em} = 440$ nm, $\tau < 1.0$ ns, Figure 3a). A dye loading efficiency of 10% was estimated by subtracting the fluorescence intensity of the supernatant from the fluorescence intensity of the original dilute $DAPI^+$ solution. Fluorescence microscopy images show blue emission from the crystals upon excitation with UV light (Figure 3b). The observed fluorescence does not change when a polarizer is used, thus confirming the non-ordered orientation of the molecular transition moments and a random distribution of dye molecules within the silica shell owing to the isotropy of the system. Furthermore, the emission occurs only from the external part of the object, as the zeolites employed in this experiment are empty.

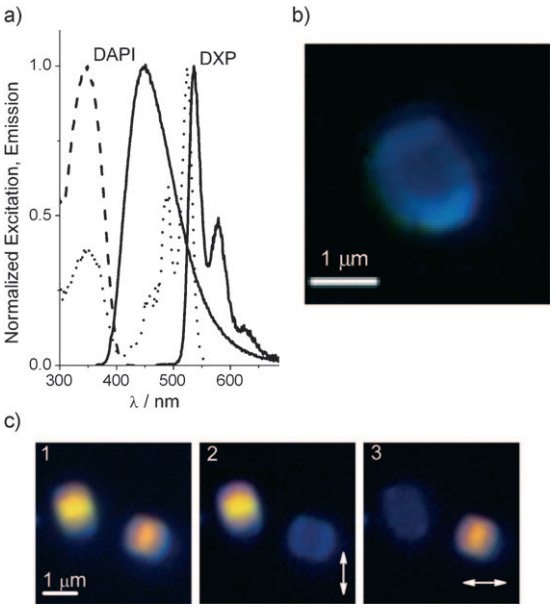

Figure 3. a) Normalized excitation (-----, •••••) and emission (——) spectra of Zeo(DXP)@PAH/PVP@SiO_2 ($\lambda_{obs} = 570$ nm, $\lambda_{exc} = 450$ nm) and Zeo@PAH/PVP@SiO_2($DAPI^+$) ($\lambda_{obs} = 440$ nm, $\lambda_{exc} = 350$ nm) crystals in toluene. b) Optical fluorescence microscopy image of a Zeo@PAH/PVP@SiO_2($DAPI^+$) crystal excited with UV light (330–385 nm). c) Optical fluorescence microscopy images of perpendicularly oriented silica-coated zeolite L crystals Zeo(DXP)@PAH/PVP@SiO_2($DAPI^+$) excited with UV light (330–385 nm). Nonpolarized (1) and polarized (2 and 3, the arrows indicate the direction of the transmitted polarization) fluorescence are shown. The scale is the same for all three images.

The same synthetic procedure was carried out with zeolite L crystals loaded with DXP molecules (Zeo(DXP)@PAH/PVP@SiO_2 in toluene; $\lambda_{em} = 536$ nm, $\tau = 3.5$ ns, Figure 3a). We chose DXP as emitter because the dye molecules arrange along the axis of the zeolite channels and their electronic transition moment is oriented in the same way. Figure 3c shows fluorescence microscopy images of two almost perpendicularly oriented Zeo(DXP)@PAH/PVP@SiO_2($DAPI^+$) crystals excited with UV light. In Figure 3c1, the Zeo(DXP)@PAH/PVP@SiO_2($DAPI^+$) crystals are excited with UV light in the absence of a polarizer. As expected, emissions of both dyes, the yellow DXP emission and the blue $DAPI^+$ fluorescence, are observed. Upon polarization of the excitation light, we always obtain emission from the $DAPI^+$ molecules entrapped in the silica shell, Figure 3c2,3. On the other hand, we observe emission from the DXP dyes entrapped in the channels of the zeolite L core only when they are able to absorb the excitation light, that is, only when the polarization of the excitation light is parallel to the crystal axis, matching the electronic transition moments of DXP (Figure 3c2,3). As expected, no energy transfer from DAPI to DXP was observed owing to the long distances

between the two dyes, which are greater than the estimated thickness of the PAH/PVP layer (5–6 nm) and than the typical values of the Förster radius of energy transfer (2–6 nm).[26]

In summary, we have developed a novel and efficient method to coat zeolite L crystals loaded with non-ionic and cationic dyes with silica, which involves initial coating with PAH and PVP and subsequent TEOS condensation. The Stöber synthesis in the presence of different dyes yields bright, luminescent, multicolor crystals with simultaneous isotropic and anisotropic intense luminescence. These crystals were analyzed using excitation and emission spectra and fluorescence microscopy with and without light polarization. The resulting core–shell structure was unambiguously confirmed through detailed TEM, SEM, and XPS investigations as well as by fluorescence analysis. UV/Vis spectroscopy showed that no leakage of the inserted dye molecules from the zeolite cores occurs, thus indicating the formation of stable and isolated capsules. Finally, we stress that the two-color system can be extended to multicolor nanomaterials; work in this direction is in progress. The dye molecules can be replaced with other systems, such as radioisotopes and paramagnetic species, thus combining the emission with other types of signaling. Functionalization of the silica surface with conventional techniques leads to the desired water- and biocompatibility for in vitro and, possibly, in vivo testing.

Experimental Section

Silica coating: All reagents were purchased from Aldrich and used without purification unless otherwise indicated. The cylindrical zeolite L crystals were prepared according to the procedure described in the literature.[19] The crystals had a mean length and mean diameter of 1.4 and 1.0 μm, respectively. Crystals loaded with non-ionic and cationic dyes were prepared by gas-phase insertion and ion exchange, respectively, with loadings around $p = 0.2$ (p is the ratio between the occupied and the total number of equivalent sites in a zeolite L crystal), as described in the literature.[6] Typically, nonloaded or loaded zeolite L crystals (5 mg) were dispersed in Milli-Q water (5 mL) and added dropwise under vigorous stirring to aqueous PAH previously sonicated for 30 min ($M_w = 15\,000$, 2 g L^{-1}, 10 mL). In the case of loaded zeolites, the PAH solution typically contained 0.05 mM dye to avoid the release of dye molecules during polyelectrolyte adsorption. Stirring was continued for 3 h, at which time the mixture was centrifuged at 4000 rpm (20 min) to eliminate excess PAH and redispersed in Milli-Q water (5 mL). The solution was mixed with aqueous PVP ($M_w = 10\,000$, 4 g L^{-1}, 10 mL) and stirred overnight. Zeta potential values of + 30 mV and + 10 mV were measured for the Zeo@PAH and Zeo@PAH/PVP samples, respectively. The mixture was centrifuged at 4000 rpm (20 min), the clear supernatant discarded, and the precipitate redispersed in ethanol (7.2 mL). Ammonia (33 wt % in water, 340 μL) was then added under vigorous stirring, and finally TEOS (3.2 μL) was added under gentle stirring. For the preparation of luminescent silica layers, the ethanol solution contained 0.05 mM dye. The mixture was allowed to react for 5 h and was centrifuged at 1000 rpm (20 min) to avoid nucleation of silica nanoparticles. Further TEOS additions were carried out to grow the silica shells.

Instrumentation: Excitation and emission spectra were measured from a suspension in spectroscopic-grade toluene in 10 mm quartz cuvettes. They were recorded with a HORIBA Jobin–Yvon IBH FL-322 Fluorolog 3 spectrofluorometer equipped with a 450 W xenon arc lamp, double-grating excitation and emission monochromators (2.0 nm mm^{-1} dispersion, 1200 grooves mm^{-1}), and a TBX-4-X single-photon-counting detector. Time-resolved measurements were performed using the time-correlated single-photon counting (TCSPC) option on the Fluorolog 3. NanoLEDs (295 or 431 nm; full width at half maximum (FWHM) < 750 ps) were used to excite the samples. The goodness of the fit was assessed by minimizing the reduced chi squared function (χ^2) and by visual inspection of the weighed residuals. Fluorescence microscopy was carried out with an Olympus BX-41 instrument equipped with a Hg high pressure lamp, air objective 100 × 1.0, UMWB2 (band pass 460–490 nm), U-MWG2 (band pass 510–550 nm), and MWU2 (band pass 330–385 nm) excitation cubes, and a color camera. TEM was carried out with a JEOL JEM 1010 transmission electron microscope operating at an acceleration voltage of 100 kV. SEM images were obtained using a JEOL JSM-6700F FEG scanning electron microscope operating at an acceleration voltage of 5.0 kV for secondary-electron imaging (SEI). XPS analysis of the samples was performed using a VG Escalab 250 ESCA instrument (VG Scientific) with aluminum Kα1.2 monochromatic radiation at 1486.92 eV. The zeta potential was determined through electrophoretic mobility measurements using a Malvern Zetasizer 2000 instrument.

Received: August 23, 2008
Published online: November 21, 2008

Keywords: core–shell materials · fluorescence · polyelectrolytes · silica · zeolites

[1] See, for example, A. D. Schlüter, *Functional Molecular Nanostructures (Topics in Current Chemistry)*, Springer, Berlin, **2005**.
[2] D. T. McQuade, A. E. Pullen, T. M. Swager, *Chem. Rev.* **2000**, *100*, 2537.
[3] See, for example, G. R. Newkome, C. N. Moorefield, F. Vögtle, *Dendrimers and Dendrons: Concepts, Syntheses, Applications*, Wiley-VCH, Weinheim, **2001**.
[4] L. A. Chrisstoffels, A. Andronov, J. M. J. Fréchet, *Angew. Chem.* **2000**, *112*, 2247; *Angew. Chem. Int. Ed.* **2000**, *39*, 2163.
[5] F. Torney, B. G. Trewyn, V. S. Y. Lin, K. Wang, *Nat. Nanotechnol.* **2007**, *2*, 295.
[6] a) G. Calzaferri, K. Lutkouskaya, *Photochem. Photobiol. Sci.* **2008**, *7*, 879; b) G. Calzaferri, S. Huber, H. Maas, C. Minkowski, *Angew. Chem.* **2003**, *115*, 3860; *Angew. Chem. Int. Ed.* **2003**, *42*, 3732.
[7] Z. Popović, M. Otter, G. Calzaferri, L. De Cola, *Angew. Chem.* **2007**, *119*, 6301; *Angew. Chem. Int. Ed.* **2007**, *46*, 6188.
[8] Z. Popović, M. Busby, S. Huber, G. Calzaferri, L. De Cola, *Angew. Chem.* **2007**, *119*, 9056; *Angew. Chem. Int. Ed.* **2007**, *46*, 8898.
[9] P. A. Anderson, R. Armstrong, P. P. Edwards, *Angew. Chem.* **1994**, *106*, 669; *Angew. Chem. Int. Ed. Engl.* **1994**, *33*, 641.
[10] S. Megelski, A. Lieb, M. Pauchard, A. Drechsler, S. Glaus, C. Debus, A. J. Meixner, G. Calzaferri, *J. Phys. Chem. B* **2001**, *105*, 25.
[11] R. Q. Albuquerque, G. Calzaferri, *Chem. Eur. J.* **2007**, *13*, 8939.
[12] H. Musso, C. Rathjen, *Chem. Ber.* **1959**, *92*, 751.
[13] a) O. Bossart, L. De Cola, S. Welter, G. Calzaferri, *Chem. Eur. J.* **2004**, *10*, 5771; b) H. Maas, G. Calzaferri, *Angew. Chem.* **2002**, *114*, 2389; *Angew. Chem. Int. Ed.* **2002**, *41*, 2284.
[14] a) A. Burns, H. Ow, U. Wiesner, *Chem. Rev.* **2006**, *106*, 1028; b) E. Rampazzo, S. Bonacchi, M. Montalti, L. Prodi, N. Zaccheroni, *J. Am. Chem. Soc.* **2007**, *129*, 14251; c) V. Sokolova, M. Epple, *Angew. Chem.* **2008**, *120*, 1402; *Angew. Chem. Int. Ed.* **2008**, *47*, 1382.
[15] L. M. Liz-Marzán, P. Mulvaney, *J. Phys. Chem. B* **2003**, *107*, 7312.
[16] Z. L. Wang, R. P. P. Gao, J. L. Gole, J. D. Stout, *Adv. Mater.* **2000**, *12*, 1938.

[17] R. Koole, M. M. van Schooneveld, J. Hilhorst, C. D. Donega, D. C. t'Hart, A. van Blaaderen, D. Vanmaekelbergh, A. Meijerink, *Chem. Mater.* **2008**, *20*, 2503.
[18] R. A. Farrell, N. Petkov, H. Amenitsch, J. D. Holmes, M. A. Morris, *J. Mater. Chem.* **2008**, *18*, 2213.
[19] A. Burns, H. Ow, U. Wiesner, *Chem. Soc. Rev.* **2006**, *35*, 1028.
[20] C. Wu, J. Zheng, C. Huang, J. Lai, S. Li, C. Chen, Y. Zhao, *Angew. Chem.* **2007**, *119*, 5489; *Angew. Chem. Int. Ed.* **2007**, *46*, 5393.
[21] G. Schneider, G. Decher, *Nano Lett.* **2004**, *4*, 1833.
[22] A. Z. Ruiz, D. Brühwiler, T. Ban, G. Calzaferri, *Monatsh. Chem.* **2005**, *136*, 77.
[23] A. Madani, A. Aznar, J. Sanz, J. M. Serratosa, *J. Phys. Chem.* **1990**, *94*, 760.
[24] I. Pastoriza-Santos, J. Pérez-Juste, L. M. Liz-Marzán, *Chem. Mater.* **2006**, *18*, 2465.
[25] L. Krasemann, B. Tieke, *Langmuir* **2000**, *16*, 287.
[26] J. R. Lakowicz, *Principles of Fluorescence Spectroscopy*, Kluwer, New York, **1999**.

